Quantitative relationship between electron transfer rate and surface microstructure of laser-modified graphite electrodes

ARTICLE *in* ANALYTICAL CHEMISTRY · AUGUST 1989

Impact Factor: 5.64 · DOI: 10.1021/ac00190a010

2 AUTHORS, INCLUDING:

Richard Mccreery
University of Alberta
177 PUBLICATIONS **9,452** CITATIONS

Quantitative Relationship between Electron Transfer Rate and Surface Microstructure of Laser-Modified Graphite Electrodes

Ronald J. Rice and Richard L. McCreery*

Department of Chemistry, The Ohio State University, 120 West 18th Avenue, Columbus, Ohio 43210

Previous investigations demonstrate that increases in electron transfer rate constant, k°, on highly ordered pyrolytic graphite (HOPG) basal plane correlate with the appearance of edge plane defects and that such defects may be created with laser or electrochemical pretreatment. In the current work both capacitance (C°_{obs}) and k°_{obs} for $Fe(CN)_6^{3-/4-}$ on HOPG were measured as functions of power density of the activating laser. Over a power density range from 0 to 130 MW cm^{-2}, k°_{obs} increased by more than 5 orders of magnitude while C°_{obs} increased by a factor of 8. Both k°_{obs} and C°_{obs} may be expressed as linear combinations of the basal and edge plane k° and C° values, weighted by the fractional coverage of edge plane on the electrode surface (f_e). Determinations of f_e from both k°_{obs} and C°_{obs} are quantitatively consistent and in both cases increase with power density above a threshold of 45 MW cm^{-2}. Although effects of surface roughness may also be involved, the results indicate that the electron transfer activity of laser-modified HOPG is predominantly dependent on edge plane density.

INTRODUCTION

The wide variation of heterogeneous electron transfer rate constants (k°) on carbon electrodes has attracted a variety of investigations into the influence of surface chemistry on charge transfer kinetics. The many factors which may affect k° on carbon have been discussed many times in the primary literature (*1–16*) and in a recent monograph (*17*). The overall motivation of these research efforts is an understanding of what aspects of the carbon surface determine k° for simple systems such as $Fe(CN)_6^{3-/4-}$ and more complex cases like O_2 reduction and many organic redox systems.

Our laboratory's approach to the problem has involved laser activation (*12, 13, 16*) of both glassy carbon (GC) and highly ordered pyrolytic graphite (HOPG) combined with Raman spectroscopy as a probe of carbon microstructure (*18, 19*). HOPG is a structurally well-characterized material whose basal plane is atomically clean when freshly cleaved. HOPG can serve as a simple model of more complicated materials such as GC, to permit insights into the structural changes which promote electron transfer. For the case of laser activation of basal plane HOPG, we showed that k° for $Fe(CN)_6^{3-/4-}$ changes suddenly with increasing laser power density, with a rate increase of approximately 5 orders of magnitude occurring after 50 MW/cm^{-2} laser treatment (*18*). This activation correlates with the formation of graphite edge plane on the original HOPG basal plane. The correlation of edge plane density and high k° was also observed for electrochemical activation of HOPG and for laser activation of edge plane HOPG and GC-20.

The 1360-cm^{-1} Raman band of carbon materials is a good marker for edge plane, with greater 1360-cm^{-1} intensity indicating smaller graphitic microcrystallites (*18, 20, 21*). The correlation is based on spectra of carbons with different basal plane lattice parameter, L_a, determined from X-ray diffraction (*20*). While the 1360-cm^{-1}/1582-cm^{-1} Raman intensity ratio is directly proportional to the reciprocal of L_a in carbon powders, it is not obvious how this quantitative proportionality applies to laser-activated HOPG. There is no reason to expect an even or narrow distribution of L_a over the activated basal plane surface or into the bulk HOPG. Although the 1360/1582 ratio will increase with edge plane density (and decreasing microcrystalline size), the relationship should be considered semiquantitative, and it would be risky to attempt to calculate edge plane density from the Raman data with useful accuracy. The objective of the work reported here was a quantitative correlation of edge plane density with electron transfer rate for laser-activated HOPG. If the qualitative conclusion that electron transfer occurs at edge plane defects is correct, then the observed rate constant should quantitatively track the edge plane density.

The approach we used to quantitatively evaluate edge plane density was originally suggested by Yeager et al. (*22–24*) and is based on capacitance measurements. Edge plane carbon has much higher capacitance per unit area, C°, than basal plane, so capacitance can serve as a measure of edge plane density in the absence of other effects. By correlating capacitance changes with k° changes caused by laser activation, we will establish a more quantitative relationship between observed k° and surface edge plane density.

EXPERIMENTAL SECTION

All solutions were prepared daily by using distilled water which was then purified with a Nanopure water purification system. Potassium ferrocyanide was used as received from Mallinckrodt Inc. for the preparation of 1 mM potassium ferrocyanide in 1 M KCl, which was then degassed for approximately 20 min with purified argon. The HOPG was a gift from Arthur Moore at Union Carbide, Parma, OH. Basal plane HOPG was mounted as described previously (*18*), with the electrode being defined by a Viton O-ring with 1 mm inside diameter. Although HOPG was cleaved in the conventional way with adhesive tape, it was noted that special care was required to avoid forming defects on the freshly cleaved surface. As will be discussed below, a small number of defects can yield a large error in the observed basal plane rate constant. Carefully cleaved and handled basal plane HOPG exhibited a ΔE_p for $Fe(CN)_6^{3-/4-}$ in 1 *M* KCl of at least 700 mV at 0.2 V/s, and smaller ΔE_p values indicated a defective surface. If localized mechanical damage occurred on the surface during cell assembly, it was possible to observe two voltammetric couples with different ΔE_p for $Fe(CN)_6^{3-/4-}$, indicating a damaged region larger than $(Dt)^{1/2}$. As a routine practice, any fresh basal HOPG surfaces exhibiting two voltammetric peaks or a single couple with $\Delta E_p < 700$ mV for $Fe(CN)_6^{3-/4-}$ were rejected and cleaved again.

Edge plane HOPG surfaces are difficult to prepare due to irregularities in how the edges are cut. It is likely that rough edges can be folded over during polishing or cleaning, leading to partial basal plane exposure. For measurements on edge plane HOPG, the sample was embedded in Torr-seal (Varian) with the edge exposed and then sanded with 600-grit silicon carbide sandpaper and polished successively with 1.0-, 0.3-, and 0.05-μm alumina before rinsing with Nanopure water.

Cyclic voltammetry experiments were performed with a Tecmar Labmaster analog interface board in a PC compatible computer which controlled an Advanced Idea Mechanics (Columbus, OH) Model 8709 potentiostat. A BAS Model RE-1 Ag/AgCl reference electrode (3 M NaCl) was used for all electrochemical experiments.

* Author to whom correspondence should be addressed.

0003-2700/89/0361-1637$01.50/0

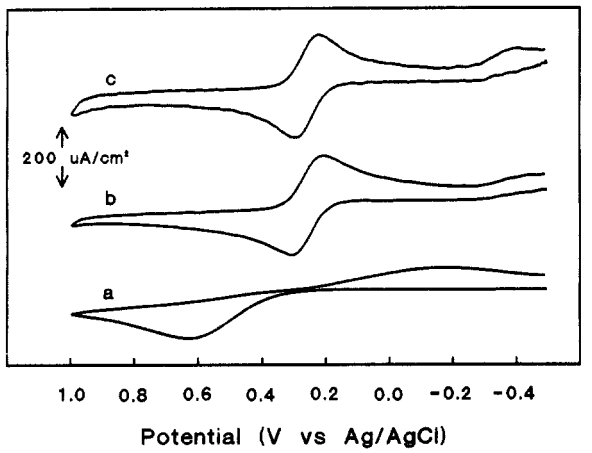

Figure 1. Cyclic voltammograms (0.2 V s^{-1}) of 1 mM $Fe(CN)_6^{3-/4-}$ in 1 M KCl on HOPG basal plane: (a) freshly cleaved; (b) after three 50 MW cm^{-2} laser pulses in air; (c) freshly cleaved surface after three 90 MW cm^{-2} laser pulses in air. Reduction at ca. −0.4 V is apparently due to dioxygen.

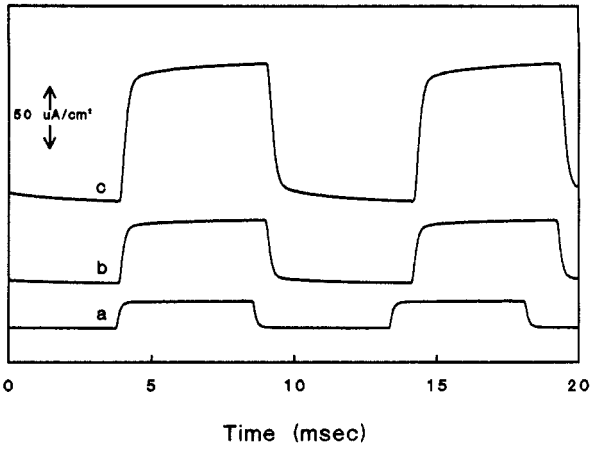

Figure 2. Raw current density waveforms for HOPG basal plane in 1 M KCl, in response to a ca. 100 Hz, 20 mV p-p triangle wave applied potential. dc potential was 0.00 V vs Ag/AgCl, electrolyte was 1 M KCl. The three E_{app} waveforms differed slightly in frequency and amplitude, but in all cases had the same value of dE/dt. Curve a is fresh HOPG, curve b is after three 50 MW cm^{-2} laser pulses, and curve c is a fresh surface after three 90 MW cm^{-2} pulses in air.

All cyclic voltammetry experiments used a scan rate of 0.2 V/s unless otherwise indicated. A platinum wire was used as an auxiliary electrode for all electrochemical experiments. A diffusion coefficient for $Fe(CN)_6^{3-}$ of 6.3×10^{-6} cm^2/s was used for analysis of all electrochemical data.

Differential capacitance measurements were made by applying a 100-Hz, 20-mV peak to peak triangle wave centered on 0.0 vs Ag/AgCl from an Exac Model 128 function generator to the electrochemical cell and recording the current response on a Tektronix Model 7854 digital oscilloscope. This method has been described and characterized by Gileadi et al. (*25*, *26*). The area of the electrode used for capacitance calculations was determined by chronoamperometry and had a typical value of 0.06 cm^2. Semiintegral analysis of voltammograms was performed by using the G1 algorithm of Oldham as described elsewhere (*27*), and $k°$ values were determined conventionally from ΔE_p by the method of Nicholson (*28*). Due to the need for extrapolation of Nicholson's working curves for $\Delta E_p > 200$ mV, $k°$ values below 10^{-4} cm s^{-1} are less accurate than those in the range of 10^{-1} to 10^{-3} cm s^{-1}.

Laser pretreatment was performed in ambient air with three 9-ns laser pulses from the beam center of a Nd:YAG laser operating at 1064 nm. Due to variations in beam quality and pulse-to-pulse variability, cited power densities are ±20%. The measured power density was found to be sensitive to laser alignment and aging, and power densities reported in a preliminary communication (*19*) were found to be erroneously low. The cell was assembled immediately after electrode activation. In situ activation in the electrochemical cell was not employed due to power density variations induced by Fresnel diffraction of laser light from the O-ring. This effect is of interest in itself but was avoided here by activating in ambient air without the O-ring present.

Electrochemical activation was conducted with a procedure similar to that of Engstrom (*5*, *6*) with a controlled potential anodization at various potentials followed by a cathodic step to −0.1 V vs Ag/AgCl for 30 s. Raman spectra were obtained with a 515-nm laser and Spex 1403 spectrometer as described previously ("gross" spectra, ref 18).

RESULTS AND DISCUSSION

The qualitative effects of laser irradiation on HOPG electron transfer kinetics, capacitance, and Raman spectra were examined initially, over a wider range of power densities than reported previously (*18*). Figure 1 shows voltammograms for $Fe(CN)_6^{3-/4-}$ on the initial HOPG basal plane and after 50 and 90 MW cm^{-2} laser irradiations. There is a large decrease in ΔE_p after the 50 MW cm^{-2} pulses and a further, but smaller, decrease at higher power density. Figure 2 shows the current waveforms resulting from a 20-mV peak-to-peak 100-Hz triangle wave potential to a blank electrolyte solution. Before laser irradiation, the waveform is a square wave, indicating

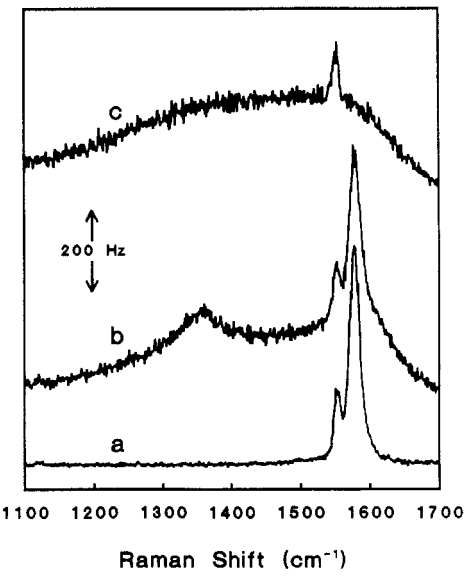

Figure 3. Raman spectra of HOPG basal plane before and after laser treatment. Raman laser was 515 nm, ca. 75 mW at sample. Laser pretreatment was the same as in Figures 1 and 2, with spectra a–c corresponding to 0, 50, and 90 MW cm^{-2} pretreatment. The small peak at 1565 cm^{-1} is due to atmospheric dioxygen and is irrelevant to the carbon results.

a nearly ideal capacitance of 1.9 μF cm^{-2}. After 50 MW cm^{-2} laser treatment the current increases slightly, with a minor increase in slope of the square wave response. At higher laser power densities (curve C), the current continues to increase, as does the slope. Raman spectra following treatment at the power densities in Figures 1 and 2 are shown in Figure 3. As noted previously (*18*, *19*), the 50 MW cm^{-2} pretreatment produces a 1360-cm^{-1} band indicating fracturing of the HOPG lattice. At high power densities, the first-order Raman bands broaden and coalesce, indicating severe disorder of the carbon lattice (*20*, *21*, *29*, *30*). Quantitative changes in $k°$ upon laser activation are indicated in Figure 4. The initial $k°$ before activation was very low on basal plane HOPG, with values below 1×10^{-7} cm s^{-1}. Significant variation in this initial rate constant was observed, probably due to adventitious defects, but it was always less than 6×10^{-7} cm s^{-1}. Laser irradiation at power densities below 45 MW cm^{-2} had no effect on the observed ΔE_p. Above 45 MW cm^{-2}, the laser treatment caused an abrupt increase in $k°$ from $<10^{-7}$ to $>10^{-3}$ cm s^{-1}. With

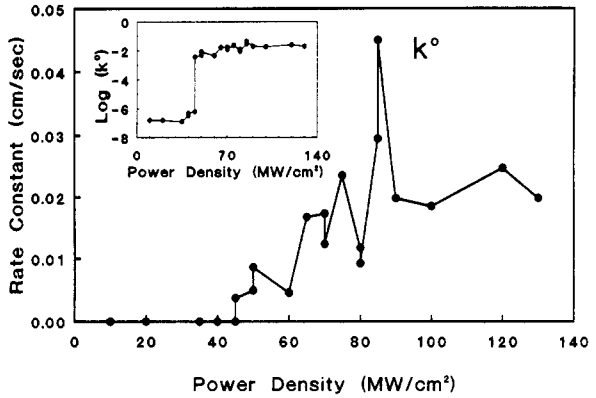

Figure 4. Observed electron transfer rate constant, $k°_{obs}$ for $Fe(CN)_6^{3-/4-}$, calculated from voltammograms similar to those in Figure 1, as a function of laser activation power density. Each voltammogram was preceded by cleavage of the HOPG basal plane and three laser pulses in air. Inset shows same data with a logarithmic ordinate.

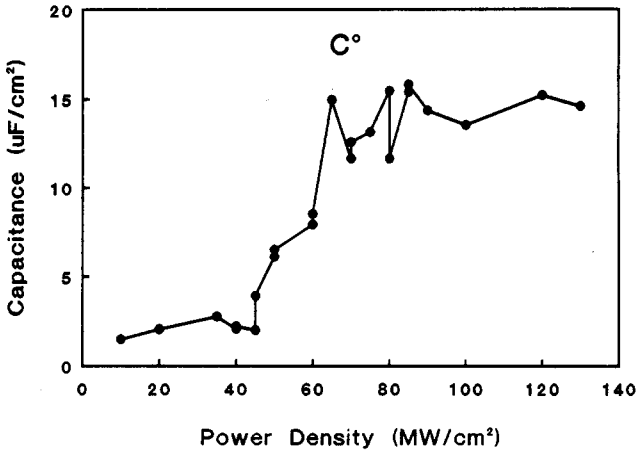

Figure 5. Observed capacitance, $C°_{obs}$, for HOPG as a function of laser power density. Surfaces prepared were as in Figure 4; electrolyte was 1 M KCl.

increasing power density, $k°$ continued to increase, reaching a plateau of about 0.02 cm s^{-1} at high power density. The significant variability in $k°$ apparent in Figure 4 probably results from variation in surface cleanliness occurring when activation is carried out in air and has been noted previously on glassy carbon (*16*). While this variation is quite large, it is small considering the 5+ order of magnitude range in $k°_{obs}$ (see inset of Figure 4). Semiintegration over the entire power range showed sigmoidal curves, indicating no observable adsorption or other unexpected effects (*27*).

The capacitance of HOPG basal plane was measured as a function of laser power density with the results shown in Figure 5. Untreated basal plane has an anomalously low capacitance of 2–3 $\mu F\ cm^{-2}$, which has been attributed to its partial semiconductor character (*14, 23, 24*). This capacitance is independent of the triangle wave frequency over a range from 10 to 1000 Hz, implying a negligible Faradaic component. Above 45 MW cm^{-2}, $C°$ increases with power density up to a plateau of ca. 15 $\mu F\ cm^{-2}$. Note that $C°$ increased by a factor of about 8 over a power density range where $k°$ increased by a factor of 10^5.

Edge plane HOPG exhibited a $C°$ of 60 $\mu F\ cm^{-2}$ and $k°$ for $Fe(CN)_6^{3-/4-}$ of 0.06 cm s^{-1} after conventional polishing and rinsing in Nanopure water. Laser activation at high power (100 MW cm^{-2}) increased $C°$ slightly to 70 $\mu F\ cm^{-2}$ and $k°$ to 0.10 cm s^{-1}. It is likely that the laser removed polishing debris and mechanical effects of polishing to yield slightly higher values of $C°$ and $k°$. While literature values for $C°$ on edge plane HOPG vary significantly, the value of 70 $\mu F\ cm^{-2}$ is within the commonly cited range (*23, 31*). Despite the variation in reported values, it is clear that edge plane HOPG has a $C°$ ca. 30 times that of basal plane. Furthermore, the edge plane $k°$ is at least 10^5 times as large as properly prepared basal plane.

The effects of electrochemical pretreatment (ECP) of basal plane HOPG on $k°$ and $C°$ were also examined, although in less detail. The apparent capacitance of the ECP surface was much higher than laser pretreated surfaces, with values of 80–150 $\mu F\ cm^{-2}$ being observed for ECP potentials of 2.1–2.5 V (2 min anodization followed by 30 s at −0.10 V). $k°$ values for these same surfaces ranged from 0.01 to 0.22 cm s^{-1}. The slopes of the nominally flat "square waves" shown in Figure 2 were much larger for ECP surfaces, consistent with a large Faradaic component of the observed capacitance. ECP has no effect on $k°$ or $C°$ at pretreatment potentials of 1.8 V or below.

It is clear from the results reported here and in the literature that the basal and edge planes of HOPG differ greatly in their electrochemical properties. It is well-known that HOPG is an anisotropic material, with the "a" (in plane) and "c" (perpendicular to plane) axes differing greatly in electrical and thermal conductivity, thermal expansion coefficient, optical properties, and tensile strength (*32, 33*). Thus it is not surprising that the $k°$ and $C°$ values reflect this anisotropy.

The qualitative changes in the HOPG surface upon laser treatment are not unexpected, based on previous work. The large decrease in ΔE_p for $Fe(CN)_6^{3-/4-}$ accompanies the appearance of the 1360-cm^{-1} Raman band and is attributable to creation of graphitic edge plane. The severe broadening of Raman bands at high power density is consistent with severe disorder of the graphitic lattice. The spectrum of Figure 3C is similar to that of amorphous carbon and certain carbon blacks, which have small L_a and L_c lattice parameters and relatively large interplanar spacing (*20, 21, 29, 30*). On the basis of the voltammetry of Figure 1, such surfaces have good electron transfer activity but have been severely altered structurally from HOPG. The increased slopes of the capacitance waveforms upon activation may be due to surface Faradaic reactions or nonideal capacitance. The increase upon 50 MW cm^{-2} treatment is slight and is much smaller than that for glassy carbon, electrochemically pretreated HOPG, or severely disordered surfaces. Such behavior has been attributed to surface redox reactions (*4, 34*), capacitance with a variety of RC time constants (*25, 26*), or incorporation of nonelectroactive cations into surface films (*35*). For the initial and 50 MW cm^{-2} surfaces, the slope is a minor contribution to the observed capacitance but does serve as an indication of nonideal capacitive behavior.

On a more quantitative basis, the large difference in $k°$ for basal vs edge plane is consistent with previous reports from our lab and others but is much larger than that reported in the 1970s. Morcos and Yeager (*15*) report a basal to edge plane ratio of $k°$ for $Fe(CN)_6^{3-/4-}$ of about 3, whereas our lab (*18, 19*) and others (*3*) observe a ratio of more than 10^5. This discrepancy is attributable to the extreme care required to avoid defects on the freshly cleaved basal plane surface. Even a small density of surface defects yields a large rate increase on basal plane, resulting in an erroneously small ratio of edge to basal plane $k°$ values. In addition, it is difficult to prepare clean edge plane surfaces, resulting in low $k°$ values and an apparent decrease in the edge/basal $k°$ ratio. It is possible that the basal plane $k°$ reported here ($<10^{-7}$ cm s^{-1}) is actually smaller, and the low observed activity is due entirely to defects.

The capacitance we observe for untreated basal plane (~2.0 $\mu F\ cm^{-2}$) is also smaller than reported values (ca. 3 $\mu F\ cm^{-2}$) (*24*). Since the ratio of edge to basal plane $C°$ is much smaller than the $k°$ ratio, the observed capacitance will be less sen-

sitive to adventitious defects. As will be shown below, an edge plane defect density of 1.6% would increase the observed basal $C°$ from 2 to 3 $\mu F\ cm^{-2}$, so it is possible the discrepancy is caused by variations in the density of unavoidable edge plane defects. Alternatively, the difference may result from the use of a different electrolyte. In either case, the discrepancy is not important to the conclusions drawn here.

The effects of laser pretreatment on basal plane $C°_{obs}$ and $k°_{obs}$ can be divided into three regions, depending on power density. Below 45 MW cm^{-2}, no effect on $k°$ is observed, and $C°$ varies slightly. Between 45 and 90 MW cm^{-2} both $k°$ and $C°$ increase, by factors of ca. 10^5 and 8, respectively. The Raman spectrum of HOPG following laser activation in this power range exhibits a 1360-cm^{-1} band indicating the formation of edge plane. Thus $k°$ and $C°$ increases correlate with the spectroscopic marker for edge plane. At power densities from 90 to 130 MW cm^{-2}, $k°$ and $C°$ have reached plateaus, showing no apparent trend with increasing power density. The Raman spectrum in this high power density region corresponds to very disordered carbon lacking a well-defined 1360/1582 intensity ratio.

It was concluded from the spectroscopic results that the mechanism of HOPG basal plane activation by laser irradiation involved the formation of edge plane on the basal plane surface (*18*). While the mechanism of edge plane formation is currently unclear, increased edge plane always produces increased $k°$. As a first approximation, it is useful to hypothesize that $k°$ is solely a function of edge plane density on HOPG, and that the observed rate constant, $k°_{obs}$, is a weighted sum of the basal and edge plane $k°$ values, as indicated by

$$k°_{obs} = k°_e f_e + k°_b(1 - f_e) \quad (1)$$

where $k°_e = k°$ for pure edge plane, $k°_b = k°$ for pure basal plane, and f_e is the fraction of electrode area which is edge plane. Equation 1 does not address the issue of why edge plane has a higher rate constant but merely states that the observed rate constant depends on f_e. Equation 1 should hold for the case where $(Dt)^{1/2}$ is large relative to both the edge plane defects and the distance between them. It is similar to the expressions derived by Amatore, Saveant, and Tessier (*36*) for partially blocked electrodes with surface coverage not too close to 1. Making the same hypothesis about observed capacitance yields

$$C°_{obs} = C°_e f_e + C°_b(1 - f_e) \quad (2)$$

where $C°_e$ is the capacitance per unit area of pure edge plane and $C°_b$ is the capacitance per unit area of pure basal plane. $C°_e$ may include a component due to surface Faradaic processes or nonideal capacitance, but the contribution of this component is assumed to be equal for any edge plane, regardless of its origin. Provided $C°_e$, $C°_b$, $k°_e$, and $k°_b$ are known, eq 1 and 2 may be used to calculate f_e for a given surface from $k°_{obs}$ and $C°_{obs}$. This approach provides two independent measurements of f_e based on both electron transfer kinetics and capacitance.

$k°_b$ is less than 10^{-7} cm s^{-1}, probably in the region of 10^{-9} cm s^{-1}. Since $k°_e$ is much larger than $k°_b$, the contribution of $k°_b$ to $k°_{obs}$ in eq 1 is negligible on laser-treated surfaces and the accuracy of $k°_b$ is unimportant for determining f_e from eq 1. The average of several $k°$ values for laser-activated edge plane HOPG yielded a value of 0.10 cm s^{-1} for $k°_e$. This result is lower than laser-treated GC by a factor of 2 but is higher than for activated basal plane. Using 10^{-7} cm s^{-1} for $k°_b$ and 0.10 for $k°_e$, f_e was calculated from eq 1 and the data of Figure 4, as a function of power density. The plot of f_e vs power density determined from $k°_{obs}$ is shown in Figure 6. Since $k°_b$ contributes negligibly to $k°_{obs}$, f_e is proportional to $k°_{obs}$. Thus the observed $k°$ is determined solely by the edge plane

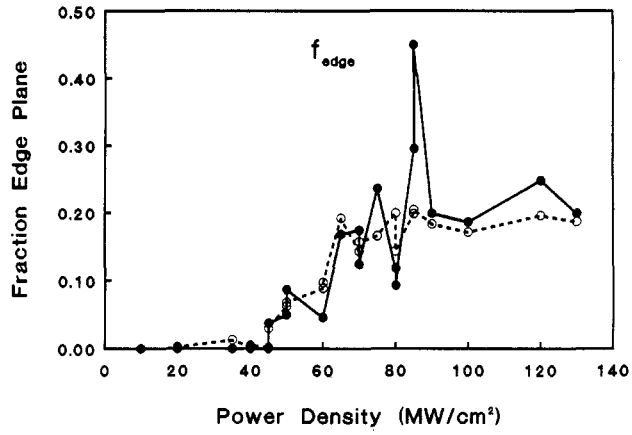

Figure 6. Plots of f_e vs power density calculated from $k°_{obs}$, $C°_{obs}$, and eq 1 and 2: closed circles, f_e calculated from data of Figure 4 and eq 1, with $k°_e = 0.10$ cm s^{-1} and $k°_b = 1 \times 10^{-7}$; open circles, f_e calculated from data of Figure 5 with $C°_b = 1.9\ \mu F\ cm^{-2}$ and $C°_e = 70\ \mu F\ cm^{-2}$.

contribution for $k°_{obs}$ greater than about 10^{-6} cm s^{-1}.

Equation 2 may be used to calculate f_e from $C°_{obs}$ as a function of power density, using values of 1.9 $\mu F\ cm^{-2}$ for $C°_b$ and 70 $\mu F\ cm^{-2}$ for $C°_e$. The results are plotted in Figure 6 on the same scale as f_e values determined from $k°_{obs}$. f_e values determined from either $k°$ or $C°$ show simiar trends with power density and agree within experimental variation. There are plateaus below 45 MW cm^{-2} and above 90 MW cm^{-2}, and there is an increase with power density in between.

The agreement among f_e values determined from independent measurements of capacitance and $k°$ is significant in light of the wide range of $k°_{obs}$ values covered and the relatively small variation in $C°_{obs}$. For example, generation of 1% edge plane on initially perfect basal plane would increase $k°_{obs}$ by a factor of at least 10^4, while $C°_{obs}$ would increase by only 37%. The quantitative correlation of $C°_{obs}$ and $k°_{obs}$ implied by the similar f_e values supports the validity of eq 1 and 2. In mechanistic terms, the results of Figure 6 imply that both capacitance and charge transfer rate are controlled by the fractional density of edge plane on the electrode surface. Thus the laser treatment of HOPG basal plane serves to increase edge plane density, as shown qualitatively in previous work, and the current results demonstrate a quantitative relationship.

A proportionality between $k°_{obs}$ and f_e, as in eq 1, permits the conclusion that electron transfer is localized on edge plane for HOPG, with the possible exception of very low $k°_{obs}$ ($<10^{-7}$ cm s^{-1}). While the association of electron transfer sites with edge plane is itself significant, it does not reveal the chemical nature of the site. There are likely to be oxygen-containing functional groups on edge plane, but several strong arguments are available against their involvement in electron transfer to $Fe(CN)_6^{3-/4-}$ or ascorbic acid, and similar common test systems (*16*, *37*). Surface oxides may be involved in more complicated redox processes such as O_2 reduction, hydrazine oxidation, and binding of large or small biological molecules, but large $k°$ values for small, presumably outer sphere electron transfers appear possible without oxygen functional groups.

The observation of a single voltammetric couple over a wide range of $k°$ values is significant with regard to the nature of the surface. The voltammograms used to calculate $k°$ values for Figure 4 had the classical shape expected for a planar electrode, implying that any surface heterogeneity occurs on a dimension that is small relative to $(Dt)^{1/2}$ (*36*). Thus the distance between exposed edge plane regions on the laser-treated surfaces must be less than a few micrometers, and the diffusion fields to these regions must overlap heavily on the voltammetric time scale. Provided $(Dt)^{1/2}$ is large compared

to the distance between edge plane sites, the voltammogram will be governed by the Nicholson–Shain treatment and eq 1 will apply. Raman results presented elsewhere (*18*) indicate an approximate average microcrystallite size on laser-treated HOPG of several hundred angstroms (*20*), indicating a spacing between edge plane sites of much less than 1 μm. Thus the activated surface is behaving like an array of small active sites closely packed in an inert plane, with an observed k° governed by eq 1. While the inert plane is very unreactive toward electron transfer, it does have capacitance, leading to the minimum observed C° for basal plane of ~ 2 μF cm^2.

It can be argued that rate and capacitance increases upon laser activation may be due to increases in microscopic surface area, since HOPG basal plane is initially very flat. Surface roughness is insufficient to explain the current results because both k°_{obs} and C°_{obs} should be proportional to roughness factor if roughness were the only variable involved. If roughness were responsible for the 10^4 increase in k°_{obs} with laser activation, there would be a 10^4 increase in capacitance, contrary to the observed results. Because some roughening is likely to accompany edge plane formation, there may be a contribution of microscopic area increases to k°_{obs} enhancement. The extent of this contribution is difficult to assess without independent measurement of microscopic surface area.

Application of these results to more commonly used carbon materials such as glassy carbon is complicated by uncertainties in the measurement of k° and C°. HOPG basal plane is clean and has a well-defined capacitance with very low contribution from surface Faradaic reactions. However, glassy carbon (GC) exhibits a large variation of C° and k° with pretreatment (*1*), in part because of surface cleanliness and the presence of surface oxides. As noted earlier, such oxides can undergo Faradaic reactions which contribute to observed "capacitance", leading to an erroneously high capacitance. The best GC surface for comparison to the present results is vacuum heat treated (VHT) GC-20, which has a capacitance of 10 μF cm^2 and appears to be free of surface redox groups (*4*). Equation 2 results in an f_e of 15% for a capacitance of 10 μF cm^2 and predicted k° of about 0.04 cm s^{-1} for $Fe(CN)_6^{3-/4-}$. The observed rate constant on VHT GC-20 is about 0.15 cm s^{-1} (*4*). It may be an oversimplification to apply the HOPG results to the microstructurally distinct GC-20 surface, but it appears that edge plane density affects C°_{obs} and k°_{obs} in similar ways on both HOPG an GC-20 surfaces.

Several recent reports from our laboratory (*12*, *16*, *37*) and from others (*3*, *4*, *38*) have noted an inverse correlation of capacitance and k° for GC-20 and pyrolytic graphite, in apparent contradiction to current results. For example, polished GC-20 may have a capacitance in the 60–100 μF cm^2 range, but this value decreases to 10 μF cm^2 upon VHT (*4*). However, the k° may increase significantly upon VHT, in contradiction to eq 1 and 2. This apparent discrepancy is very likely attributable to the involvement of surface oxides on polished GC surfaces. Such oxides may make a large (even dominant) contribution to C°_{obs}, but have minor or negative effects on k° for simple systems (*16*). Thus removal of oxides by VHT or laser treatment may greatly reduce C°_{obs} while having minor or positive effects on k°_{obs}. Similar arguments can be made about surface impurities, since they may have a larger effect on k°_{obs} than C°_{obs}. Equations 1 and 2 will be valid when edge plane density is the major variable determining C°_{obs} and k°_{obs}, and the main point of this paper is the effect of laser treatment and carbon microstructure on f_e. If other variables such as surface cleanliness or oxides are important, such as on most glassy carbon surfaces, eq 1 and 2 would not be expected to apply. In particular, it is possible to increase k°_{obs} while reducing C°_{obs} on GC-20 by removing impurities and surface oxides. In the case of HOPG, the initial surface is oxide free, and the base-line C°_{obs} is free of Faradaic contributions.

ACKNOWLEDGMENT

The authors thank Robert Bowling for assistance with Raman spectra and Arthur Moore of Union Carbide for providing HOPG samples.

LITERATURE CITED

(1) Hu, I. F.; Karweik, D. H.; Kuwana, T. *J. Electroanal. Chem.* **1985**, *188*, 59.
(2) Hu, I-F.; Kuwana, T. *Anal. Chem.* **1986**, *58*, 3235.
(3) Wightman, R. M.; Deakin, M. R.; Kovach, P. M.; Kuhr, W. G.; Stutts, K. J. *J. Electrochem. Soc.* **1984**, *131*, 1578.
(4) Fagan, D. T.; Hu, I. F.; Kuwana, T.; *Anal. Chem.* **1985**, *57*, 2759.
(5) Engstrom, R. C.; Strasser, V. A. *Anal. Chem.* **1985**, *56*, 136.
(6) Engstrom, R. C. *Anal. Chem.* **1982**, *54*, 2310.
(7) Cabaniss, G. E.; Diamantis, A. A.; Murphy, W. R., Jr.; Linton, R. W.; and Meyer, T. J. *J. Am. Chem. Soc.* **1985**, *107*, 1845.
(8) Wang, J.; Hutchins, L. O. *Anal. Chim. Acta* **1985**, *167*, 325.
(9) Gonon, F. G.; Fombarlet, C. M.; Buda, M. J.; Pujol, J. F. *Anal. Chem.* **1981**, *53*, 1386.
(10) Wightman, R. A.; Palk, E. C.; Borman, S.; Dayton, M. A. *Anal. Chem.* **1978**, *50*, 1410.
(11) Kepley, L. J.; Bard, A. J. *Anal. Chem.* **1988**, *60*, 1459.
(12) Poon, M.; McCreery, R. L. *Anal. Chem.* **1986**, *58*, 2745.
(13) Poon, M.; McCreery, R. L. *Anal. Chem.* **1987**, *59*, 1615.
(14) Randin, J.-P. In *Encyclopedia of Electrochemistry of the Elements*, Bard, A. J., Ed.; Dekker: New York, 1976; Vol. 7, pp 12–21, 238–239.
(15) Morcos, I.; Yeager, E. *Electrochim. Acta* **1970**, *15*, 953.
(16) Poon, M.; McCreery, Richard L.; Engstrom, R. *Anal. Chem.* **1988**, *60*, 1725.
(17) Kinoshita, K. *Carbon: Electrochemical and Physical Properties*, Wiley: New York, 1988; Chapter 5.
(18) Bowling, R. J.; Packard, R. T.; McCreery, R. L. *J. Am. Chem. Soc.* **1989**, *111*, 1217.
(19) Bowling, R. J.; Packard, R. T.; McCreery, R. L. *J. Electrochem. Soc.* **1988**, *135*, 1605.
(20) Tuinstra, F.; Koenig, J. L. *J. Chem. Phys.* **1970**, *53*, 1126.
(21) Dresselhaas, M. S.; Dresselhaas, G. *Adv. Phys.* **1981**, *30*, 139.
(22) Randin, J. P.; Yeager, E. *J. Electroanal. Chem.* **1972**, *36*, 257.
(23) Randin, J. P.; Yeager, E. *J. Electrochem. Soc.* **1971**, *118*(15), 711.
(24) Randin, J. P.; Yeager, E. *J. Electroanal. Chem.* **1975**, *58*, 313.
(25) Gileadi, E.; Tshernikovski, N. *Electrochim. Acta* **1971**, *16*, 579.
(26) Gileadi, E.; Tshernikovski, N.; Babai, M. *J. Electrochem. Soc.* **1972**, *119*(8), 1018.
(27) Bowling, R.; McCreery, R. L. *Anal. Chem.* **1988**, *60*, 605.
(28) Nicholson, R. S. *Anal. Chem.* **1965**, *37*, 1351.
(29) Vidano, R.; Fischbach, D. B. *J. Am. Ceram. Soc.* **1978**, *61*, 13.
(30) Nakamizo, M.; Kammereck, R.; Walker, P. L. *Carbon* **1974**, *12*, 259.
(31) Reference 17, p 294.
(32) Autio, G. W.; Scala, E. *Carbon* **1968**, *6*, 41.
(33) Macia, G. *Carbon* **1987**, *25*, 837.
(34) Oren, Y.; Soffer, A. *J. Electroanal. Chem.* **1985**, *186*, 63.
(35) Nagaoka, et al. *Anal. Chem.* **1988**, *60*, 2766.
(36) Amatore, C.; Saveant, J.; Tessier, D. *J. Electroanal. Chem.* **1983**, *147*, 39.
(37) Bowling, R. J.; Packard, R. T.; McCreery, R. L. *Langmuir* **1989**, *5*, 683.
(38) Bodalbhai, L.; Brajter-Toth, A. *Anal. Chem.* **1988**, *60*, 2557.

RECEIVED for review January 4, 1989. Accepted May 1, 1989. This work was supported by the Air Force Office of Scientific Research and by the donors of the Petroleum Research Fund, administered by the American Chemical Society. Raman instrumentation was developed under the support of The Chemical Analysis Division of the National Science Foundation.